

PAPER • OPEN ACCESS

## A Numerical Study of fluid flow and Pressure Drop analysis of Catalytic Converter using Commercial CFD code

To cite this article: Aniket Patil *et al* 2019 *IOP Conf. Ser.: Earth Environ. Sci.* **312** 012032

View the [article online](#) for updates and enhancements.

A promotional banner for the 240th ECS Meeting. The banner features a colorful striped border at the top. On the left, the ECS logo is displayed in a green circle. To its right, the text reads "240th ECS Meeting" in large blue font, followed by "Oct 10-14, 2021, Orlando, Florida" in a smaller blue font. Below this, it says "Register early and save up to 20% on registration costs" in bold black font, and "Early registration deadline Sep 13" in a smaller black font. At the bottom left, there is a red "REGISTER NOW" button. On the right side of the banner, there is a photograph of a diverse group of people in professional attire, smiling and clapping, suggesting a successful event or presentation.

**ECS** **240th ECS Meeting**  
Oct 10-14, 2021, Orlando, Florida  
**Register early and save  
up to 20% on registration costs**  
Early registration deadline Sep 13  
**REGISTER NOW**

# A Numerical Study of fluid flow and Pressure Drop analysis of Catalytic Converter using Commercial CFD code

Aniket Patil<sup>1</sup>, Mayuresh Takale<sup>1</sup>, Bageerathan Thirunavukkarasu<sup>1</sup>, Thundil Karuppa Raj R<sup>1\*</sup>

<sup>1</sup> School of Mechanical Engineering, VIT University, Vellore, Tamil Nadu, INDIA - 632014

\*Corresponding author email id – [thundilr@gmail.com](mailto:thundilr@gmail.com)

**ABSTRACT:** In recent years catalytic converter is a necessary device to achieve low emissions in all the vehicles. This study of the after treatment device is to understand the fluid flow and to optimize the design. It is important to know the pressure drop taking place inside the catalytic converter in order to design the catalytic converter. In this paper, a numerical study has been conducted to study the effect of fluid flow inside the catalytic converter and effect of change in geometry using commercial CFD tool. The working fluid considered in this study is air. A 3D simulation is carried out having straight inlet pipe and with change in inlet pipe angle of the catalytic converter. The monolith substrate region is modeled as a porous medium. The governing equations namely conservation of mass, momentum are used for solving the analysis. The analysis involved determining pressure variation across the geometry of the converter system for different mass flow rates and change inlet pipe angle. The numerical results were used determine the pressure drop across the substrate and the flow characteristics inside the catalytic converter. The numerical study shows good conformance with the experimental results with maximum deviation of error 2.54% for straight inlet pipe configuration. The effect of change in inlet pipe angle, effect of inlet cone angle and effect of splitting the substrate into sections are also presented.

*Keywords:* Catalytic converter, Pressure Drop, CFD analysis, substrate, ANSYS CFX, monolith.

## 1. Introduction

In recent past decade automotive emission standards have become stricter and there are different methods and efforts have been presented to find the cause of emissions and the development of new technologies for controlling and regulating the emissions. An Automotive catalytic converter usually made of a round shaped or oval shaped substrate encased in a metallic shell. The monolith substrate is having tubular channels along the length and connected to the exhaust system through inlet and outlet



cones. Different methodologies and efforts are investigated in the recent years which will use the maximum volume of the catalytic converter. The design of any after treatment device is largely depends upon the pressure drop occurring in the device. The reason behind that is when your pressure drop is more than back pressure is created on engine exhaust gas and engine performance gets affected. So it is important to know the pressure drop occurring in catalytic converter. The uniform flow distribution assures the maximum utilisation of the catalyst volume inside the catalytic converter. Therefore, most modern catalytic converters have configuration geometry having inlet and outlet pipe, inlet and outlet cone, long substrate to ensure smooth uniform flow between these different cross sections. J. S. Howitt and T. C. Sekella [1] have experimentally conducted durability studies on monolithic catalytic converters having cylindrical geometry with symmetric cone profiles. They performed the test on the engines with dynamometer but not on the on-road actual vehicle test. They found that the ability of the converter to reach the active temperature and capability of the converter to convert high percentage of the pollutants has more influence on the effectiveness of the converter. They suggested that the small angle deflectors can result in balanced flow profile where the effectiveness is increased. A. P. Martin et al., [2] investigated the performance of catalytic converter under different conditions of flow distributions. CFD techniques were utilised to model the maldistribution of aging and light off conversion performing steady tests. They have conducted emission testing on a vehicle throughout ECE and EUDC test cycles. They found insignificant effects on later stages of ECE cycle. Kwangsup Hwang et al., [3] has conducted dynamic flow studies on the catalytic converter with flow visualization techniques. They studied the flow patterns of the normal flow conditions using Laser Doppler Velocimetry and other visualization techniques. They found that the geometry of the catalytic converter influences the effective surface area of the converter. Also the space between the catalyst brick has influenced the result. Seokhwan Lee et al., [4] conducted the studies on the catalytic converters by varying the engine loading conditions from no-load to full-load conditions. They found that the temperature beyond 1050 degree Celsius can spoil the characteristics of the catalyst in the converter. The increase in the misfire has added up temperature to the exhaust gas which ruins the catalyst in catalytic converter. Yong-Seok Cho et al., [5] has developed an alternative method to control the emissions from the catalytic converter by Cranking Exhaust Gas Ignition method. This method uses the unburnt mixture to flow through the catalytic converter for 10 seconds and the mixture is burnt with the help of glow plugs. The thermal energy released during the operation has warmed up the catalyst and efficiency is increased. They also found that the warm-up process can be faster by using a leaner air-fuel mixture. Exhaust emissions were controlled when this method was used. Gregory et al., [6] conducted the emission studies on the tuned exhaust of a four-cylinder engine. Two coupled catalyst is used in this study and comparative studied were carried out with single catalyst system. Under steady state conditions, both the catalyst performs the same. During higher flow rate conditions, the peak flow rate remains the same. The authors have found that the catalyst sizing influences the efficiency of the system. Onorati et al., [7] has conducted 1D modeling of flow reactions in pre-catalyst and main catalyst using a numerical model GASDYN. The chemical reactions were taken into account along with the thermal as well as mass transfer. The influence of insulating mat and cerium oxides has also been considered. The catalyst contains two close coupled pre-catalyst along with a main catalyst where the simulated results were in good agreement with the experimental results. Soo-Jin Jeong and Woo-Seung Kim [8] has conducted 3D numerical study on the warm-up catalyst with the emission performance. Compressible flow with unsteady conditions was considered to analyse the impact of the warm-up catalyst over the main catalyst and emissions of the tail pipe. The authors have found that the early warming of the catalyst has no effect on the exhaust gas. The main catalyst has less efficiency during the early warm up period, which is increased with gradual hot exhaust gas flow. Jinke Gong et al., [9] considered a three way catalyst to perform the study on the monolith geometric parameters on influencing the emission conversion characteristics. The authors have used the commercial CFD code

FLUENT to solve the governing equations by considering the chemical reaction mechanisms. The decrease in the ratio of the elliptical geometry model has efficient catalytic conversion results. They found that the increment in length of the converter has better conversion efficiency. The catalyst with higher surface area and lesser wall thickness has better conversion rates and efficient. Bassem H. Ramadan et al., [10] has conducted a study on the character of the internal flow in the catalytic converter. The authors have used the CFD technique to perform the 3D calculations of the flow through the catalytic converter. The authors have conducted experimentation on the catalytic converter to study the flow analysis, velocity profile at various locations. The author has found that the geometry profile has influence over the effectiveness of conversion in device. The authors have considered the back pressure, mass flow, aspect ratios, and inlet and outlet cone angles and offset conditions. The profile over the angled pipe configuration has non-uniform flow conditions; increase in mass flow conditions had influenced the uniform flow conditions. The author has found that the increase in the cone angle has increased the pressure drop. Xiaogang Zhang and Paul Tennison [11] investigated a numerical three dimensional fluid flow and pressure drop characteristics for the catalytic converter geometry of two substrate inside. They carried out this study for different positions of two substrate considered and air gap width between them. The study shows the effects of relative positions of flow uniformity inside the catalytic converter with two substrates. Julia Windmann et al., [12] investigated and predicted tail pipe emissions based on numerical simulation of catalytic converter. They carried out three dimensional transient numerical studies showing the influence of velocity in front of inlet face of three way catalytic converter. They investigated and discussed the differences of chemical behaviour and thermal behaviour because of the shape and velocity distribution. Sophie Salasc et al., [13] carried out a study that aims on highlighting the impact of inlet manifold design on flow distribution focussing on different manifold designs configurations. The results obtained shows good trends with the design of closed coupled catalytic converter and manifold for improved emission performance. Thundil Karuppa Raj R. and Ramsai R [14] have conducted numerical analysis of flow of fluid in the catalytic converter using commercial CFD code. They assumed air as the working fluid. The authors have considered a rotationally symmetric geometry model with a porous medium to analyze the effect of inlet pipe angle. They have validated the numerical results with the experimental results from literature. The authors have varied the mass flow rates and inlet pipe angles to study the back pressure across the converter. These results were used to effectively design the catalytic converter to perform at maximum efficiency. Soo-Jin Jeong and Woo-Seung Kim [15] study shows the light of performance of monolith catalytic converter with reduced pressure loss to both balanced space velocity and usage of geometric surface area of the channels. The study also shows thermal durability based on thermal shock parameter, the cell combined shows weaker thermal resistance than conventional monolith.

## **2. Motivation and Objective:**

Catalytic converter is an after treatment device which is widely used in automotive industries to achieve lower levels of emissions. With the use of the device pressure drop takes place across the porous zone which is modelled with catalyst materials for chemical reaction. The porous zone thus offers frictional effects and there is a loss of velocity and pressure drop takes place across the length of substrate. This causes back pressure on the exhaust gas which is entering into the catalytic converter. So in this case the engine has to more work in order to remove out the exhaust from the tail pipe. So the pressure drop analysis becomes essential. The good optimal design of a catalyst inside catalytic converter needs a good trade-off between the pressure drop and flow uniformity in the monolith substrate. This numerical analysis is not considered with respect to chemical behaviour inside the catalytic converter but it concerns with pressure drop analysis across the substrate. This numerical study involves computational simulations to perform three dimensional calculations inside the catalytic converter using CFD.

### 3. Numerical Methodology:

#### 3.1 Geometry & modeling:

The design configuration considered for this numerical study is shown in figure 1. The substrate is considered is having circular cross section. A typical catalytic converter consists of catalyst substrate, mat-insulation material, and metallic outer cell. The porous zone which is a monolith substrate consists of 350 channels per square inch. Here the pressure drop study is carried out by changing the inlet pipe cone angle. Figure 1 (b) and figure 1 (c) shows the truncated inlet geometrical configuration at 45° and 60° respectively. Working fluid considered is air and it is at 873K. Following Table 1 shows the dimensions of the of zero degree inlet geometry.

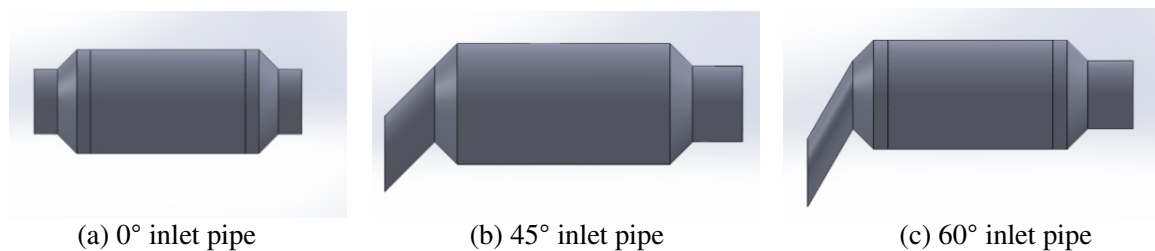


**Figure 1.** Three dimensional model configuration of with 45° cone angle.

**Table 1.** Dimensions of the geometry considered 0° inlet pipe

| Section                   | Dimensions   |
|---------------------------|--------------|
| <b>Inlet</b>              | 1.875 inches |
| <b>Cone Angle</b>         | 45°          |
| <b>Substrate Diameter</b> | 3 inches     |
| <b>Substrate Length</b>   | 4.5 inches   |
| <b>Pipe Length</b>        | 1.24 inches  |

#### 3.2 Discretization:

All the 3-D geometries are modelled in solid works 14 software and meshed in ICEM CFD 18.1 pre-processing software tool. The entire domain is discretized by using hexagonal mesh elements. The reason behind is hexagonal mesh gives accurate results and it involves less computational efforts. The geometry is divided into main four parts namely inlet and outlet pipe, inlet and outlet cone and porous zone or monolith substrate for the sake of this numerical study. The minimum determinant quality of 30% is considered to be better for the meshed geometry and minimum angle. The maximum angle for ICEM CFD meshing is 44.19° maintained with a maximum determinant quality of 82.8 %. Number of nodes are around 1262144 and number of elements are 1232065.

#### 3.3 Mathematical modeling – solving technique:

The Shear stress transport model is used in this study. The 3-D analysis is based on steady conditions and considering conservation of mass, momentum and energy using ANSYS code. ANSYS CFX 18.1 is used as solver in this work. All the governing equations are shown in (1), (2), (3) and (4) respectively. The simulations are done based on steady flow conditions. The convergence criterion for the solution is set under specific value decided by user and those criteria are normalized to absolute residual pressure drops below  $10^{-4}$ . The fluid considered is isothermal condition and so heat transfer effects are neglected. The flow in the inlet section and outlet section is turbulent type. The monolith substrate which is a porous

medium and the flow inside porous medium is considered as laminar in nature. The hydraulic diameter of the channel is about 1.167 mm for 350 cpsi and the corresponding Reynolds number results in a laminar flow inside the substrate. So the flow inside the porous zone can be considered as laminar flow. The modelling of monolith substrate is done by two resistances called linear and quadratic resistances. From figure 2 [14] linear and quadratic resistances are calculated to model the substrate inside catalytic converter using Darcy's relation from the experimental data.

**Table 2.** Experimental pressure drop across substrate

| Mass flow rate(g/sec) | Superficial Velocity(u)(m/sec) | Pressure Drop(Pa) |
|-----------------------|--------------------------------|-------------------|
| 10                    | 5.4                            | 690               |
| 20                    | 10.77                          | 1400              |
| 40                    | 21.38                          | 2900              |
| 80                    | 42.1                           | 6160              |
| 110                   | 57.16                          | 8800              |
| 150                   | 76.59                          | 12550             |
| 190                   | 95.27                          | 16500             |
| 220                   | 108.8                          | 19560             |
| 250                   | 121.9                          | 22700             |

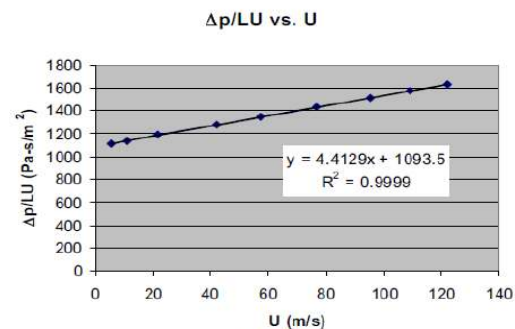


**Figure 2.** Plot of  $\Delta p / (LU)$

Conservation of mass:

$$\nabla \cdot (\rho \mathbf{V}) = 0 \quad (1)$$

Conservation of x-momentum:

$$\nabla \cdot (\rho u \mathbf{V}) = -\frac{\partial p}{\partial x} + \frac{\partial T_{xx}}{\partial x} + \frac{\partial T_{xy}}{\partial y} + \frac{\partial T_{xz}}{\partial z} + \rho \cdot g \quad (2)$$

Conservation of y-momentum:

$$\nabla \cdot (\rho v \mathbf{V}) = -\frac{\partial p}{\partial y} + \frac{\partial T_{xy}}{\partial x} + \frac{\partial T_{yy}}{\partial y} + \frac{\partial T_{yz}}{\partial z} + \rho \cdot g \quad (3)$$

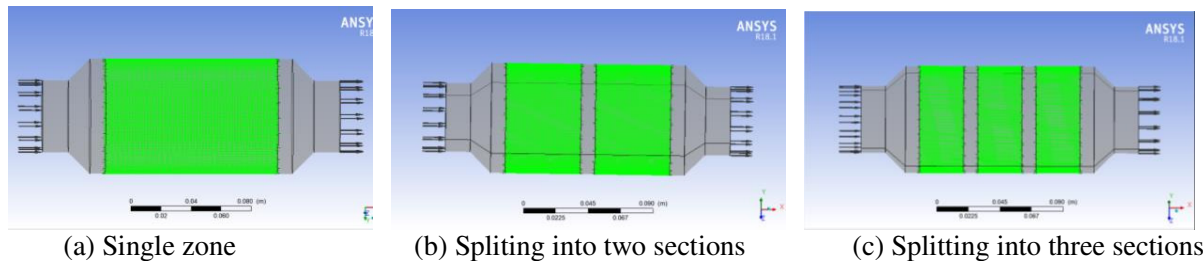
Conservation of z-momentum:

$$\nabla \cdot (\rho w \mathbf{V}) = -\frac{\partial p}{\partial z} + \frac{\partial T_{xz}}{\partial x} + \frac{\partial T_{yz}}{\partial y} + \frac{\partial T_{zz}}{\partial z} + \rho \cdot g \quad (4)$$

The experimental values of pressure drop from zero degree inlet pipe angles are shown in table 2 [14]. These values are considered for conformance to the validation of this numerical study. Assuming the walls to be having smooth surface. Radiation effects and buoyancy effects are neglected during the analysis.

### 3.4 Boundary conditions and simulation:

The catalytic converter simulation is done in ANSYS CFX software 18.1. In CFX-Pre, the various domains of the catalytic converter such as monolith substrate, fluid, substrate wall are defined. The mass flow rates are varied for each inlet pipe angle geometry and the numerical analysis is carried out. Mass flow rate is applied at the inlet section of catalytic converter. The simulations are done based on steady flow conditions. Outlet section is kept at zero relative pressure condition. The linear and quadratic resistances required are calculated using Figure 2. Figures 3 (a), (b) and (c) shows substrate section and modelling configuration and splitting configurations considered for analysis. In post-processing phase, the results of the numerical study has been carried out which include the velocity contours, pressure contours, 3D flow characterises.



(a) Single zone (b) Splitting into two sections (c) Splitting into three sections  
**Figure 3.** Catalytic converter with  $0^\circ$  inlet pipe configurations showing modeling of porous zones

#### 4. Validation, Results and Discussion:

##### 4.1 Effect of change inlet pipe angle and inlet cone angle:

This CFD numerical study shows that the pressure drop occurs to be 699.66 Pa. If the mass flow rate at inlet increases then pressure drop also increases. The computational model results good conformance with the experimental value shown in table 3 with maximum deviation around 2.54 %. For  $0^\circ$  inlet section and 150 g/sec mass flow rate the pressure drop across the substrate found to be 12303.94 Pa. Table 3 shows pressure drop values for  $0^\circ$  inlet pipe angle calculated numerically varying mass flow rates.

**Table 3.** Numerical pressure drop across substrate at  $0^\circ$  inlet pipe angle.

| Inlet pipe Angle | Mass flow rate (g/sec) | Pressure at substrate inlet (Pa) | Pressure at substrate outlet (Pa) | Pressure drop across substrate (Pa) |
|------------------|------------------------|----------------------------------|-----------------------------------|-------------------------------------|
| $0^\circ$        | 10                     | 720.999                          | 21.3324                           | 699.66                              |
|                  | 20                     | 1504.08                          | 80.8137                           | 1423.98                             |
|                  | 80                     | 7293.52                          | 1284.95                           | 6008.59                             |
|                  | 150                    | 17340.2                          | 5036.26                           | 12303.94                            |

Tables 4 and 5 show the pressure drop values of  $45^\circ$  and  $60^\circ$  inlet pipe angle configuration respectively for the corresponding mass flow rates. It can be seen that there is no any significant change in pressure drops.

**Table 4.** Numerical pressure drop across substrate at  $45^\circ$  inlet pipe angle.

| Inlet pipe Angle | Mass flow rate (g/sec) | Pressure at substrate inlet (Pa) | Pressure at substrate outlet (Pa) | Pressure drop across substrate (Pa) |
|------------------|------------------------|----------------------------------|-----------------------------------|-------------------------------------|
| $45^\circ$       | 10                     | 685.275                          | 20.7929                           | 664.4821                            |
|                  | 20                     | 1356.86                          | 80.4807                           | 1276.37                             |
|                  | 80                     | 6870.77                          | 1225.13                           | 5645.64                             |
|                  | 150                    | 15976.1                          | 4128.28                           | 11847.82                            |

**Table 5.** Numerical pressure drop across substrate at  $60^\circ$  inlet pipe angle.

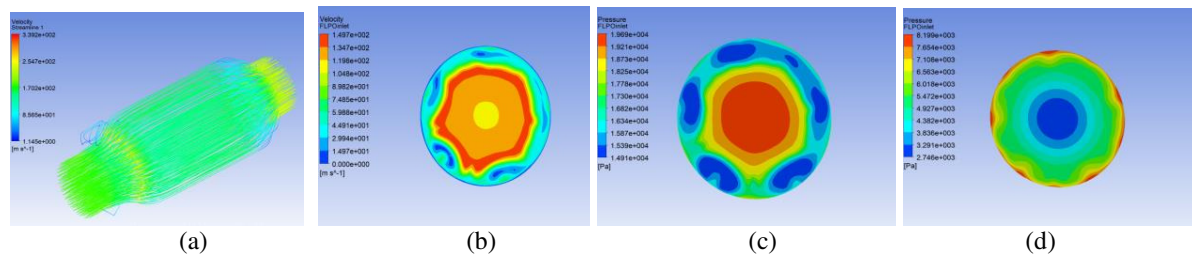
| Inlet pipe Angle | Mass flow rate (g/sec) | Pressure at substrate inlet (Pa) | Pressure at substrate outlet (Pa) | Pressure drop across substrate (Pa) |
|------------------|------------------------|----------------------------------|-----------------------------------|-------------------------------------|
| $60^\circ$       | 10                     | 664.534                          | 22.0482                           | 642.48                              |
|                  | 20                     | 1292.56                          | 87.8615                           | 1204.7                              |
|                  | 80                     | 6747.6                           | 944.223                           | 5803.37                             |
|                  | 150                    | 15737.6                          | 3127.49                           | 12610.11                            |

Table 6 shows the numerical analysis of  $0^\circ$  inlet pipe angle with  $60^\circ$  inlet cone configuration. It is found that there is no significant difference in the pressure drop as compared to experimental values of  $45^\circ$  inlet cone angle.



**Table 6.** Numerical pressure drop across substrate at 0° degree inlet pipe angle & 60° inlet cone angle.

| Inlet Cone Angle | Mass flow rate (g/sec) | Pressure at substrate inlet (Pa) | Pressure at substrate outlet (Pa) | Pressure drop across substrate (Pa) |
|------------------|------------------------|----------------------------------|-----------------------------------|-------------------------------------|
| 60°              | 10                     | 726.593                          | 25.9275                           | 700.66                              |
|                  | 20                     | 1529.88                          | 100.375                           | 1429.505                            |
|                  | 80                     | 7866.39                          | 1597.71                           | 6268.68                             |
|                  | 150                    | 18739.4                          | 6076.32                           | 12662.68                            |



**Figure 4.** (a) Fluid flow and streamline characteristics of 0° inlet pipe angle geometry at 150 g/sec, (b) Velocity distribution at substrate inlet of 0° inlet pipe angle geometry at 150 g/sec, (c) Pressure distribution at substrate inlet of 0° inlet pipe angle at 150 g/sec, (d) Pressure distribution at substrate outlet of 0° inlet pipe angle at 150 g/sec

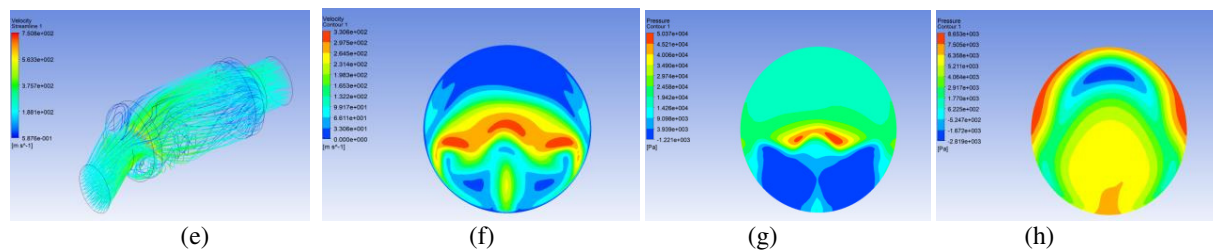


**Figure 5.** (e) Fluid flow and streamline characteristics of 45° inlet pipe angle geometry at 150 g/sec, (f) Velocity distribution at substrate inlet of 45° inlet pipe angle geometry at 150 g/sec, (g) Pressure distribution at substrate inlet of 45° inlet pipe angle at 150 g/sec, (h) Pressure distribution at substrate outlet of 45° inlet pipe angle at 150 g/sec

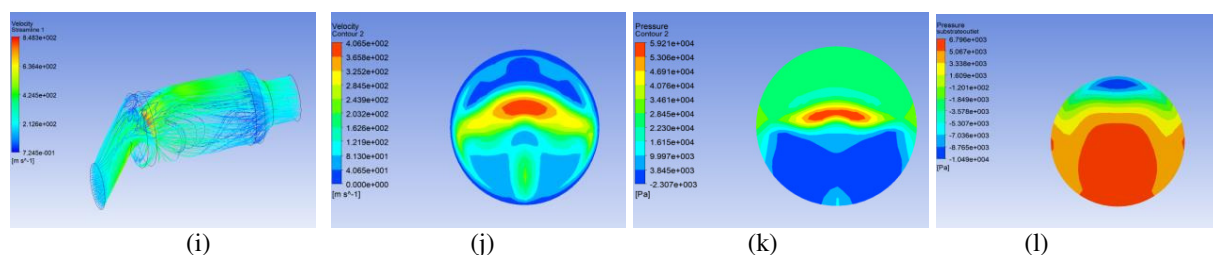


**Figure 6.** (i) Fluid flow and streamline characteristics of 60° inlet pipe angle geometry at 150 g/sec, (j) Velocity distribution at substrate inlet of 60° inlet pipe angle geometry at 150 g/sec, (k) Pressure distribution at substrate inlet of 60° inlet pipe angle at 150 g/sec, (l) Pressure distribution at substrate outlet of 60° inlet pipe angle at 150 g/sec



For 45° and 60° inlet pipe angle configuration velocity distribution for the mass flow rate of 150 g/sec is shown in figure 5 (f) and figure 6 (j) respectively. The flow inside the truncated inlet configuration is non-uniform and that can be seen from figure 5 (e) and figure 6 (i) which show the streamline characteristics. It is found that for low mass flow rate the flow found to be uniform. But for increased mass flow rate the non-uniformity of the flow increases. The velocity distribution at inlet of substrate shows maximum velocity occurs at middle portion and at the periphery velocity is zero due to no slip condition. Towards peripheral surface velocity drops down to zero. As mass flow rate increases pressure drop across the substrate increases. The experimental and numerical pressure drop values are good conformance with each other and figure 7 (a) shows the variation of pressure drop across the substrate with mass flow rate. There is no any significant change in pressure drop across the substrate is observed with the change in inlet pipe angle. Figure 7 (b) shows the variation of pressure drop values with change in inlet pipe angle. It can be seen that there is not much difference in pressure drop due to change in inlet pipe and inlet cone angle.

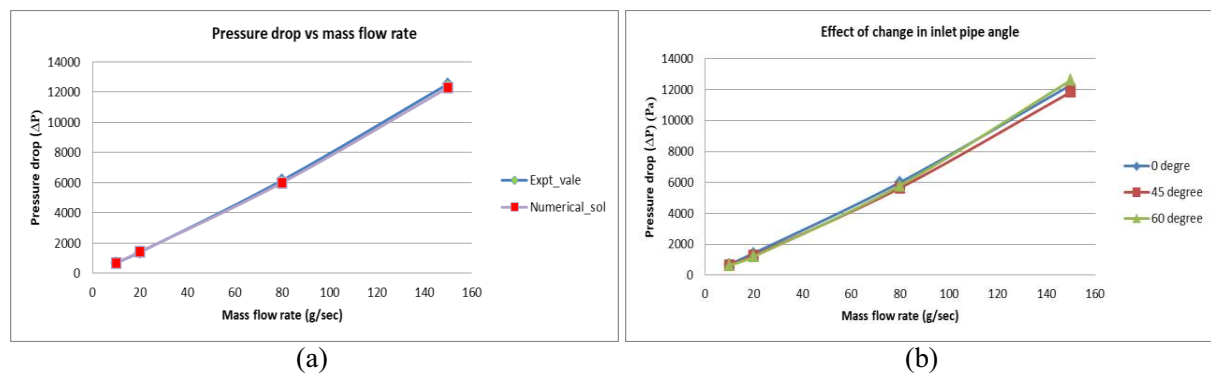


**Figure 7.** (a) Variation of pressure drop with mass flow rate (b) Effect of change in inlet pipe angle to pressure drop

#### 4.2 Effect of splitting the substrate with air gap:

Further analysis is carried out by dividing the substrate into two and three sections maintaining all the same dimensions as shown in figure 8. It can be seen that maintaining air gap between substrate sections shows decrease in pressure drop. Table 7 shows the pressure drop across the substrate when the porous zone is splitted into two substrates section as shown in figure 3 (b). It can be observed that as splitting the single substrate into two sections pressure drop across the total section decreases. A 10 mm air gap width between the each substrate section is maintained and length of each substrate is kept 52.15 mm of length. It can be seen that for a mass flow rate of 10 g/sec pressure drop reduced by 60.0977 Pa. Table 7 shows the corresponding decreased in pressure drop values for different mass flow rates.

**Table 7.** Numerical pressure drop across substrate at 0° inlet pipe angle with 45° inlet cone.

| Inlet pipe Angle | Mass flow rate (g/sec) | Pressure at substrate inlet (Pa) | Pressure at substrate outlet (Pa) | Pressure drop across substrate (Pa) |
|------------------|------------------------|----------------------------------|-----------------------------------|-------------------------------------|
| 0°               | 10                     | 660.508                          | 20.9457                           | 639.5623                            |
|                  | 20                     | 1383.32                          | 80.2657                           | 1303.0543                           |
|                  | 80                     | 6833.83                          | 1274.29                           | 5559.54                             |
|                  | 150                    | 15618.3                          | 4950.34                           | 10667.96                            |

Table 8 shows the pressure drop across the substrate when the porous zone is splitted into three substrate zones as shown in figure 3 (b). It can be observed that as splitting the single substrate into three sections pressure drop across the total section decreases. A 10 mm air gap width between the each substrate

section is maintained and length of each substrate is kept 31.4333 mm of length. It can be seen that for a mass flow rate of 10 g/sec pressure drop reduced by 123.4866 Pa. Table 8 shows the corresponding decreased in pressure drop values for different mass flow rates.

**Table 8.** Numerical pressure drop across substrate at 0° inlet pipe angle with 45° inlet cone.

| Inlet pipe Angle | Mass flow rate (g/sec) | Pressure at substrate inlet (Pa) | Pressure at substrate outlet (Pa) | Pressure drop across substrate (Pa) |
|------------------|------------------------|----------------------------------|-----------------------------------|-------------------------------------|
| 0°               | 10                     | 600.185                          | 21.0116                           | 579.1734                            |
|                  | 20                     | 1261.01                          | 80.4355                           | 1180.574                            |
|                  | 80                     | 6293.8                           | 1274.61                           | 5019.19                             |
|                  | 150                    | 14539.7                          | 4950.79                           | 9588.91                             |

Figure 8 shows the decrease in pressure drop across the total substrate when it is a single substrate, two substrate and three substrates configuration.

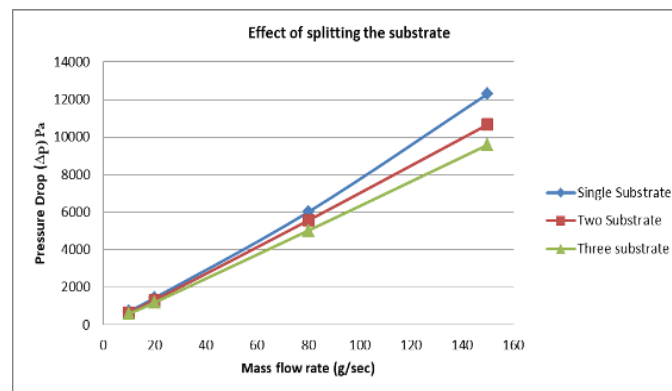


**Figure 8.** Effect of splitting the substrate into sections

## 5. Conclusion:

The numerical simulation of pressure drop and flow analysis was completed successful in ANSYS CFX. The simulation results agree with experimental values. The results show that pressure drop geometry has significant effect on flow distribution inside the catalytic converter monolith substrate. In addition to this the flow in the catalytic converter with inlet angles appears to be less uniform. The effect of change in inlet pipe angle and inlet cone angle is studied. As the mass flow rate increases pressure drop across the substrate increases. The flow tends to be more uniform if the angles are closer to inlet cone. As the mass flow rate increases flow non uniformity also increases. It is also found that changing the inlet pipe angle and cone angle does not affect the pressure drop much. So it can be taken as positive side for changing the shape of exhaust manifold as per the space availability from engine to catalytic converter. The effect of splitting the porous zone is presented which shows decrease of the pressure drop across the substrate.

## 6. Nomenclature:

|            |   |                                   |
|------------|---|-----------------------------------|
| $\dot{m}$  | - | Mass flow rate, g/sec             |
| $P$        | - | Pressure, Pa                      |
| $T$        | - | Temperature, K                    |
| $U$        | - | Superficial velocity, m/s         |
| $\rho$     | - | Density of air, kg/m <sup>3</sup> |
| $\Delta P$ | - | Pressure drop, Pa                 |
| $L$        | - | Substrate length, mm              |

## 7. References:

- [1] Howitt J.S. and Sekella T.C., Flow Effects in Monolithic automotive Catalytic Converters, SAE paper 740244, (1974)
- [2] Martin AP, Will NS, Bordet A, Cornet P, Gondoin C, Mouton X. Effect of flow distribution on emissions performance of catalytic converters. SAE transactions. 1998 Jan 1:384-90.
- [3] Hwang K., Lee K., Mueller J., Stuecken T., Schock H. and Lee J.C., Dynamic Flow Study in a Catalytic Converter Using LDV and High Speed Flow Visualization, SAE paper 950786, (1995)
- [4] Lee S., Bae C., Lee Y. and Han T., Effects of Engine Operating Conditions on Catalytic Converter Temperature in an SI Engine, SAE paper 2002-10-1677, (2002)
- [5] Cho Y.S., Lee Y.S., Kim D.S., Jung S.Y. and Ohm I.Y., An Alternative Method for Fast Light-Off of Catalysts – Cranking Exhaust Gas Ignition, SAE paper 2002-01-1678, (2002)
- [6] Gregory D., Read M., Campbell B., Inman G., Nice G., Hims R., Rabinowitz H., Tauster S., and Collin T., Emissions Implications of a Twin Close Coupled Catalyst System Designed for Improved Engine Performance on an In-line 4 Cylinder Engine, SAE paper 2001-01-1092, (2002)
- [7] Onorati A., Ferrari G., and Derrico G., 1 D Unsteady Flows with Chemical Reactions in the Exhaust Duct- System of SI Engines: Predictions and Experiments, SAE paper 2001-01-0939, (2001)
- [8] Jeong S.J., and Kim W.S., Three-Dimensional Numerical Study on the Use of Warm-up Catalyst to Improve Light- Off Performance, SAE paper 2000-01-0207, (2000)
- [9] Jinke Gong, Longyu Cai, Weiling Peng and Jingwu Liu, Yunqing Liu, Hao Cai and Jiaqiang E, Analysis to the Impact of Monolith Geometric Parameters on Emission Conversion performance Based on an Improved Threeway Catalytic Converter Simulation Model, SAE paper 2006-32-0089 (2006)
- [10] Bassem H. Ramadan and Philip C. Lundberg, Characterization of a Catalytic Converter Internal Flow, SAE paper, 2007-01-4024 (2007)
- [11] Zhang X, Tennison P. Numerical Study of Flow Uniformity and Pressure Loss Through a Catalytic Converter with Two Substrates. SAE Technical Paper; 2008 Apr 14.
- [12] Windmann J, Braun J, Zacke P, Tischer S, Deutschmann O, Warnatz J. Impact of the inlet flow distribution on the light-off behavior of a 3-way catalytic converter. SAE transactions. 2003 Jan 1:713-23.
- [13] Salasc S, Barrieu E, Leroy V. Impact of manifold design on flow distribution of a close-coupled catalytic converter. SAE Technical Paper; 2005 Apr 11.
- [14] Thundil Karupparaj R, Ramsai R. Numerical study of fluid flow and effect of inlet pipe angle In catalytic converter using CFD. Research Journal of Recent Sciences ISSN. 2006:2277-502.
- [15] Jeong SJ, Kim WS. A study on the optimal monolith combination for improving flow uniformity and warm-up performance of an auto-catalyst. Chemical Engineering and Processing: Process Intensification. 2003 Nov 1;42(11):879-95.